Dynamic behavior of Josephson-junction qubits: crossover between Rabi oscillations and Landau–Zener transitions

S.N. Shevchenko[1,2], A.S. Kiyko[1], A.N. Omelyanchouk[1], and W. Krech[2]

[1]*B. Verkin Institute for Low Temperature Physics and Engineering of the National Academy of Sciences of Ukraine, 47 Lenin Ave., Kharkov 61103, Ukraine*

[2]*Friedrich Schiller University, Institute for Solid State Physics Helmholtzweg 5, D-07743 Jena, Germany*
E-mail:sshevchenko@ilt.kharkov.ua

We study the dynamic behavior of a quantum two-level system with periodically varying parameters by solving numerically the master equation for the density matrix. Two limiting cases are considered: multiphoton Rabi oscillations and Landau–Zener transitions. The approach is applied to the description of the dynamics of superconducting qubits. In particular, the case of the interferometer-type charge qubit with periodically varying parameters (gate voltage or magnetic flux) is investigated. The time-averaged energy level populations are calculated as functions of the qubit's control parameters.

PACS: 03.67.Lx, 03.75.Lm, **74.50.+r**, 85.25.Am

1. Introduction

The quantum two-level system is a model to describe a number of physical objects such as atoms, quantum dots, molecular magnets, etc. The system can be excited from the ground state to the upper state by changing in time its parameters (due to external fields). If the parameters vary adiabatically slowly, the excitation mechanism is called Landau–Zener (LZ) transition [1,2]; if the amplitude of the field is small and its frequency is comparable to the level distance, Rabi oscillations occur [3,4]. Thus the occupation of the levels in a two-state system can be controlled by several parameters, e.g., by amplitude and frequency of an external field [5].

Recently, the two-level model was used to describe Josephson-junction systems [6], i.e., both charge qubits [7] and flux qubits [8]. The subject of the present work is the investigation of the dynamic behavior of superconducting qubits with periodically swept parameters, which is important from the point of view of state control and readout. We will relate our results to some other articles concerning the resonant excitation of a two-level system [9–13] which has been shown to

be relevant for superconducting qubits, too [14–17]. Particularly, we will describe the dynamic behavior of the interferometer-type charge qubit [18–21].

To study theoretically the dynamic behavior of a Josephson qubit, we make use of the master equation for the density matrix rather than the Schrödinger equation because this allows one to take into account both relaxation and nonzero-temperature effects. (However, in this paper we will assume the zero-temperature limit, because we are interested in the influence of relaxation processes only on the qubit dynamics.)

The diagonal components of the density matrix give the probabilities of finding the system in the respective states of the basis in which the density matrix is presented. Thus, in executing the calculations we ought to deal with a particular basis. Our calculations are mostly carried out in the stationary basis $\{|-\rangle, |+\rangle\}$ of the eigenstates of the Hamiltonian $\hat{H}^{(0)}$ in the absence of time-dependent terms. We do that for two reasons. First, it is convenient to describe Rabi oscillations and multiphoton transitions. Second, in the case of the charge qubit these states $\{|-\rangle, |+\rangle\}$ are eigenstates of the current operator, which is related to the experimentally measurable values [21]. The important point

is that we can get the occupation probability of any state provided we know the probabilities for the states in a particular basis. To demonstrate this, we will change over from the stationary basis to the so-called adiabatic basis (consisting of the instantaneous eigenstates of the time-dependent Hamiltonian $\hat{H}$) to describe the LZ effect. We emphasize that the results presented are valid for the description of any two-level system with periodically swept parameters, particularly, of a superconducting qubit. In a Josephson-junction qubit the gate voltage or the magnetic flux can be modulated periodically.

The paper is organized as following. In Sec. 2 the basic equations are presented. In Sec. 3 we study multiphoton processes and LZ transitions in a two-level system with time-dependent parameters. We apply the respective results to the phase-biased charge qubit in Sec. 4.

2. The basic equations

We start from the Hamiltonian of a two-level system (see e.g. Ref. 6)

$$\hat{H}^{(0)} = -\frac{B_x^{(0)}}{2}\hat{\sigma}_x - \frac{B_z^{(0)}}{2}\hat{\sigma}_z \qquad (1)$$

in the basis of «physical» states $\{|0\rangle, |1\rangle\}$, where $\hat{\sigma}_z|0\rangle = |0\rangle$, $\hat{\sigma}_z|1\rangle = -|1\rangle$, $\hat{\sigma}_{x,y,z}$ are the Pauli matrices. The «physical» states are the eigenstates of the Hamiltonian $\hat{H}^{(0)}$ for $B_x^{(0)}/B_z^{(0)} \to 0$. In the case of a charge qubit, these states correspond to a definite number of Cooper pairs on the island. For a flux qubit, they correspond to a definite direction of the current circulating in the ring. The Hamiltonian (1) is diagonalized by means of the matrix

$$\hat{S} = \exp\left(i\frac{\lambda}{2}\hat{\sigma}_y\right) = \begin{bmatrix} \cos\lambda/2 & \sin\lambda/2 \\ -\sin\lambda/2 & \cos\lambda/2 \end{bmatrix},$$

where

$$\sin\lambda = -\frac{B_x^{(0)}}{\Delta E}, \quad \cos\lambda = \frac{B_z^{(0)}}{\Delta E}, \quad \Delta E = \sqrt{B_x^{(0)2} + B_z^{(0)2}}.$$

The eigenstates $|-\rangle$ and $|+\rangle$ of the time-independent Hamiltonian $\hat{H}^{(0)}$ are connected with the initial basis:

$$\begin{bmatrix} |-\rangle \\ |+\rangle \end{bmatrix} = \hat{S}\begin{bmatrix} |0\rangle \\ |1\rangle \end{bmatrix}$$

Next, we introduce the time-dependent terms into the Hamiltonian (1),

$$\hat{H}^{(0)} \to \hat{H} = \hat{H}^{(0)} + \hat{H}^{(1)}(t).$$

We consider two situations,

$$(a): B_x = B_x^{(0)}, \quad B_z = B_z(t) = B_z^{(0)} + B_z^{(1)}(t), \quad (2)$$

$$(b): B_z = B_z^{(0)}, \quad B_x = B_x(t) = B_x^{(0)} + B_x^{(1)}(t), \quad (3)$$

where the time-independent/dependent terms are marked with $(0)/(1)$ indices. Making use of the transformation $\hat{H}' = \hat{S}^{-1}\hat{H}\hat{S}$, we get the Hamiltonian $\hat{H}'$ in the energy representation $\{|-\rangle, |+\rangle\}$ corresponding to these cases:

$$\hat{H}_a' = -\frac{\Delta E}{2}\hat{\tau}_z - \frac{B_z^{(1)}(t)}{2}(\sin\lambda\hat{\tau}_x + \cos\lambda\hat{\tau}_z), \quad (4)$$

$$\hat{H}_b' = -\frac{\Delta E}{2}\hat{\tau}_z - \frac{B_x^{(1)}(t)}{2}(\cos\lambda\hat{\tau}_x - \sin\lambda\hat{\tau}_z). \quad (5)$$

For convenience, we use different notations for the Pauli matrices, $\hat{\sigma}_i$ and $\hat{\tau}_i$, which operate in the bases $\{|0\rangle, |1\rangle\}$ and $\{|-\rangle, |+\rangle\}$, respectively.

We emphasize that after the substitution

$$B_x^{(1)}(t) \to B_z^{(1)}(t) \qquad (6)$$

$$B_z^{(0)} \to -B_x^{(0)}$$

$$B_x^{(0)} \to B_z^{(0)}$$

the problem (b) coincides with problem (a). This transition from Eq. (5) to Eq. (4) corresponds to a $\pi/2$ rotation about the y-axis.

To unify expressions (4) and (5) to get the equations for numerical calculations, we write down the Hamiltonian $\hat{H}'$ as following:

$$\hat{H}' = \frac{A}{2}\hat{\tau}_x + \frac{C}{2}\hat{\tau}_z. \qquad (7)$$

The quantum dynamics of our two-level system can be characterized within the standard density-matrix approach [22]. The time-evolution of the total system composed of the two-level system and the reservoir is described by the Liouville equation. After tracing over the reservoir variables, the Liouville equation can be simplified to the so-called master equation for the reduced density matrix $\hat{\rho}$. It can be written in the form

$$\hat{\rho} = \frac{1}{2}\begin{bmatrix} 1 + Z & X - iY \\ X + iY & 1 - Z \end{bmatrix}$$

which ensures the condition $\text{Tr}\hat{\rho} = 1$. The effect of relaxation processes in the system due to the weak coupling to the reservoir can be described phenomenologically with the dephasing rate Γ_φ and the relaxation rate Γ_{relax}[23]. Then the master equation takes the form of Bloch equations [22]:

$$\frac{dX}{dt} = -CY - \Gamma_\varphi X, \qquad (8)$$

$$\frac{dY}{dt} = -AZ + CX - \Gamma_\varphi Y, \qquad (9)$$

$$\frac{dZ}{dt} = AY - \Gamma_{\text{relax}}(Z - Z(0)). \qquad (10)$$

(Throughout the paper we set $\hbar = 1$.) From these equations we get $Z(t)$ which defines the occupation probability of the upper level $|+\rangle$, $P_+(t) = \rho_{22}(t) = \frac{1}{2}(1 - Z(t))$. We choose the initial condition to be $X(0) = Y(0) = 0$, $Z(0) = 1$, that corresponds to the system in the ground state $|-\rangle$. We have calculated the time evolution of $P_+(t)$ (which is essential, e.g., for the snapshot measurements [24]) as well as the time-averaged probability $\overline{P}_+$ (which is essential, e.g., for the impedance measurement technique [25]). We note that the asymptotic expression, $P_+(t)|_{t \to \infty}$, is periodic in time with the period $T = 2\pi/\omega$ of the time-dependent term of the Hamiltonian $\hat{H}^{(1)}(t)$ (see Sec. 12 of Ref. 5).

3. Non-stationary effects in a two-level system

3.1. Rabi oscillations

Hereafter we will treat the problem (a) (see Eq. (2)), making use of the following notations:

$$\hat{H} = \Delta\hat{\sigma}_x + x(t)\hat{\sigma}_z, \quad x(t) = x_{\text{off}} + x_0 \sin \omega t \quad (11)$$

with

$$B_x^{(0)} = -2\Delta, \ B_z^{(0)} = -2x_{\text{off}}, \ B_z^{(1)}(t) = -2x_0 \sin \omega t. \qquad (12)$$

This reformulation is convenient for comparing our results with the results of other papers [9–12]. Then the Hamiltonian (4) can be rewritten:

$$\hat{H}' = -\frac{\Delta E}{2}\hat{\tau}_z + x_0 \sin \omega t \cdot \hat{V}, \qquad (13)$$

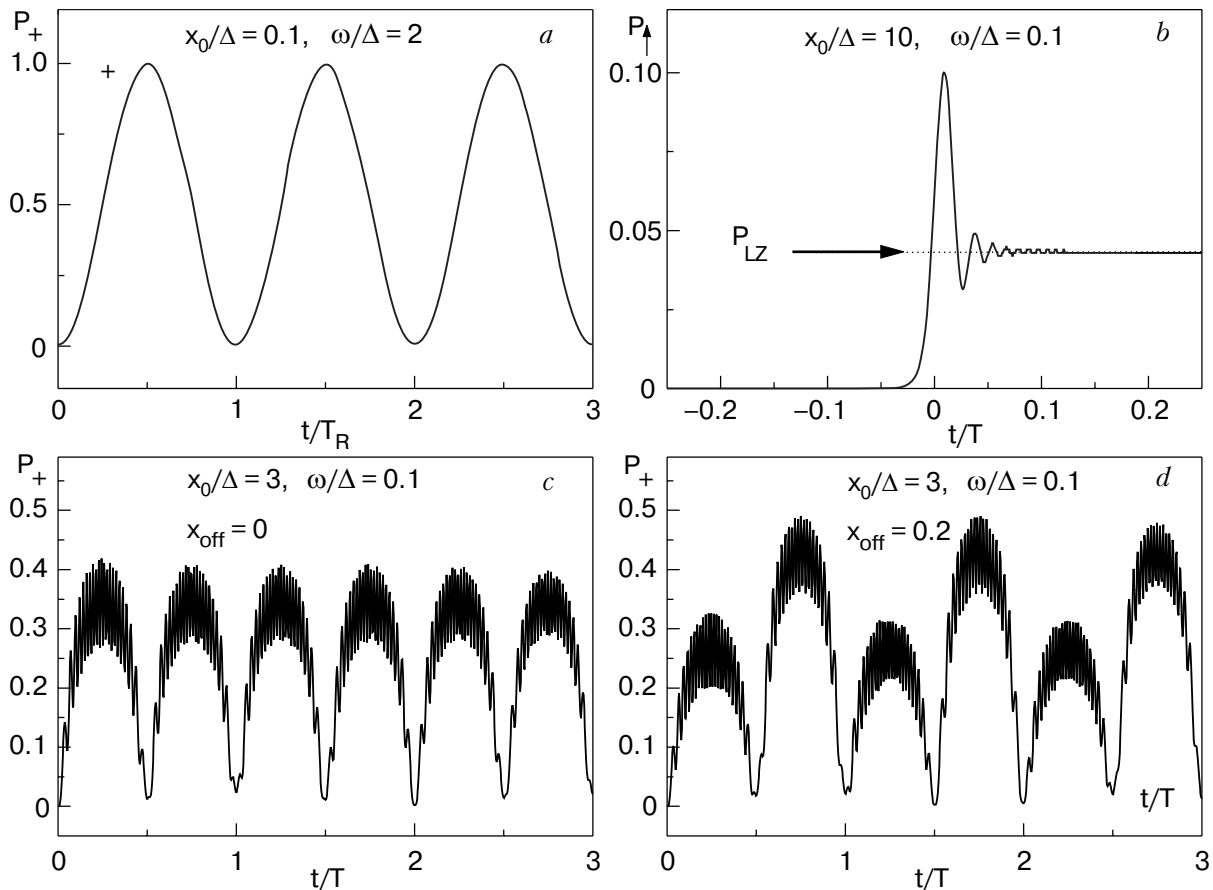$$\hat{V} = \frac{2\Delta}{\Delta E}\hat{\tau}_x - \frac{2x_{\text{off}}}{\Delta E}\hat{\tau}_z.$$

Fig. 1. Time dependence of upper-level occupation probabilities. Rabi oscillations in P_+ with the period $T_R = 2\pi/x_0$ (a), LZ transition in $P_\uparrow$ (see Sec. 3.2.) (b), P_+ probability evolution in the case of periodically swept parameters at $x_{\text{off}} = 0$ and $x_{\text{off}} \neq 0$ (c) and (d). Here $\Gamma_\varphi = \Gamma_{\text{relax}} = 0$; $T = 2\pi/\omega$.

First consider the situation $x_{\text{off}} = 0$, then the difference between the stationary energy levels is $\Delta E = 2\Delta$. In the case

$$\Delta\omega \equiv \omega - \Delta E \ll \Delta E \quad \text{and} \quad x_0 \ll \Delta E, \quad (14)$$

one can use the so-called rotating wave approximation, and the result is [26]

$$P_+(t) = \frac{1}{2}\frac{x_0^2}{x_0^2 + (\Delta\omega)^2}\left(1 - \cos\sqrt{x_0^2 + (\Delta\omega)^2}\,t\right). \quad (15)$$

For the average probability, it follows

$$\overline{P}_+ = \frac{1}{2}\frac{x_0^2}{x_0^2 + (\Delta\omega)^2}. \quad (16)$$

This means that at $\omega = \Delta E$ there is resonance, $\overline{P}_+ = \frac{1}{2}$, and $P_+(t)$ is an oscillating function with the frequency x_0. This is illustrated in Fig. 1,*a*. The width of the peak at $\omega = \Delta E$ of the $\overline{P}_+ - \omega$ curve at the half-maximum (i.e., at $P_+ = 1/4$) is approximately $2x_0$ (see the upper panels of Fig. 2).

Resonant excitations of a two-level system for $x_0/\Delta E \ll 1$ may occur not only at $\omega = \Delta E$. In the K-th order approximation, $(x_0/\Delta E)^K$, resonances exist at $\omega \simeq \Delta E/K$ [4,27]. For $x_{\text{off}} = 0$, the resonances occur at odd K only. The dependence of P_+ on time in the vicinity of K-th resonance is described by a relation similar to Eq. (15) (with substitutions $\Delta\omega \to \Delta\omega^K \simeq$ $\simeq K\omega - \Delta E$ and $x_0 \to x_0^K$). Hence, the width of the K-th resonance is of the order of x_0^K. In the resonance, $\Delta\omega^{(K)} = 0$, the energy levels $|-\rangle$ and $|+\rangle$ are equally populated so that $\overline{P}_+(\omega = \omega^{(K)} \simeq \Delta E/K) = 1/2$, which is the maximum value of $\overline{P}_+$, since the population inversion in a two-level system is not possible.

When $x_{\text{off}} \neq 0$, the matrix $\hat{V}$ has nonzero diagonal elements (see Eq. (13)). The appearance of the nonzero diagonal elements does not influence Rabi resonances at odd K, but rather results in the generation of the resonances at even K. This is demonstrated in Fig. 2 and discussed in Sec. 3.3.
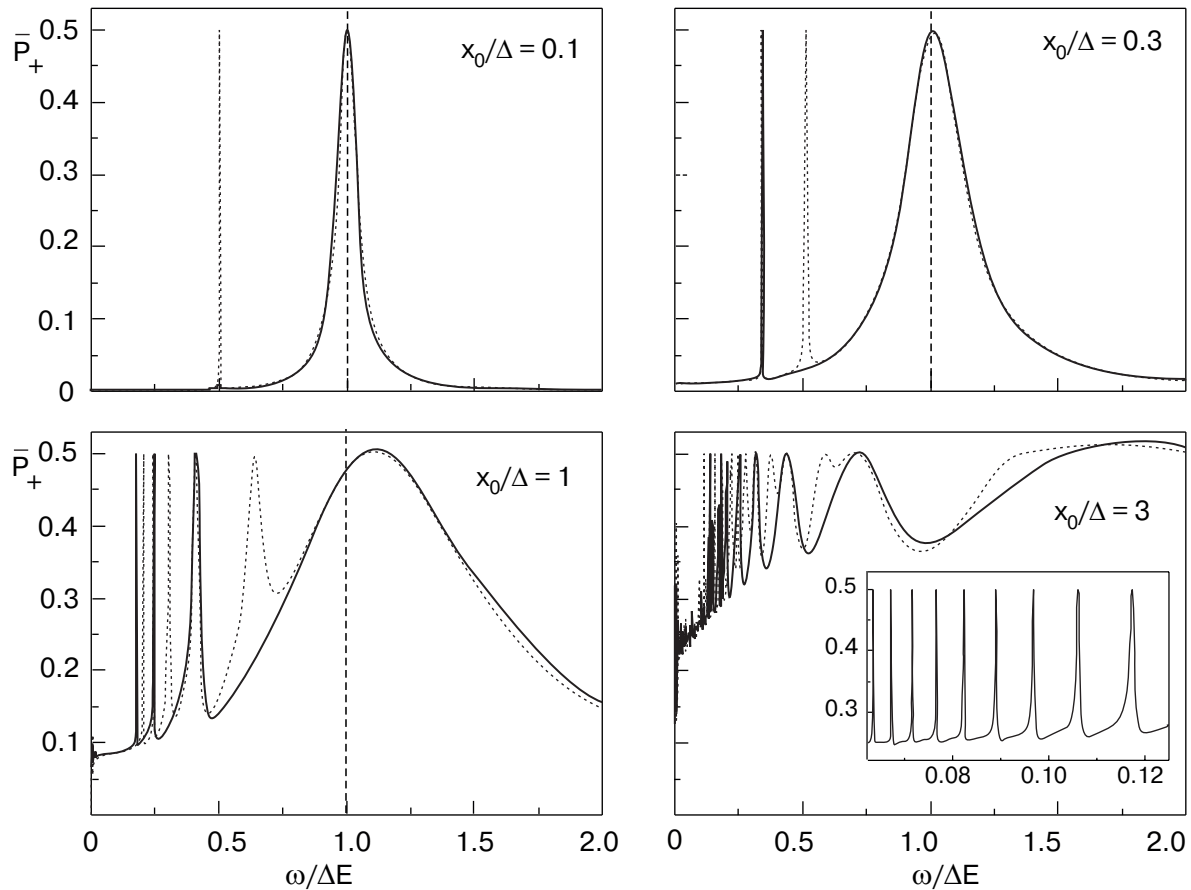

Fig. 2. Dependence of the probability $\overline{P}_+$ on the frequency ω for different x_0 at $\Gamma_\varphi = \Gamma_{\text{relax}} = 0$ and at $x_{\text{off}} = 0$ (solid line) and $x_{\text{off}} = 0.2\Delta$ (dashed line). (Only the first few resonant peaks are plotted; the others, which are very narrow, are not shown at the graphs.) Inset: enlargement of the low-frequency region.

3.2. LZ effect

The LZ effect manifests in the non-adiabatic transition with the probability

$$P_{LZ} = \exp\left(-\frac{\pi\Delta^2}{\omega x_0}\right) \qquad (17)$$

between two adiabatic energy levels during a single-sweep event [1].

The time-dependent Hamiltonian $\hat{H}$ is diagonalized in the adiabatic basis, denoted as $\{|\downarrow\rangle, |\uparrow\rangle\}$, by the $\hat{S}_1$ matrix,

$$\hat{S}_1 = \begin{bmatrix} \cos\frac{\eta}{2} & \sin\frac{\eta}{2} \\ -\sin\frac{\eta}{2} & \cos\frac{\eta}{2} \end{bmatrix},$$

$$\sin\eta = -\frac{B_x}{\Delta E_1} = \frac{2\Delta}{\Delta E_1},$$

$$\cos\eta = \frac{B_z}{\Delta E_1} = -\frac{2x(t)}{\Delta E_1},$$

$$\Delta E_1(t) = 2\sqrt{\Delta^2 + x(t)^2}.$$

The instantaneous eigenvalues of $\hat{H}$ are $E_{\downarrow,\uparrow} = \pm\Delta E_1(t)/2$.

We now can change over from the stationary basis to the adiabatic one,

$$\begin{bmatrix} |\downarrow\rangle \\ |\uparrow\rangle \end{bmatrix} = \hat{S}_1 \begin{bmatrix} |0\rangle \\ |1\rangle \end{bmatrix} = \hat{S}_1 \hat{S}^{-1} \begin{bmatrix} |-\rangle \\ |+\rangle \end{bmatrix} \equiv \hat{S}_2 \begin{bmatrix} |-\rangle \\ |+\rangle \end{bmatrix}.$$

Assuming $x_{\text{off}} = 0$, we obtain

$$\hat{S}_2 = \frac{1}{\sqrt{2}} \begin{bmatrix} \cos\frac{\eta}{2} + \sin\frac{\eta}{2} & -\cos\frac{\eta}{2} + \sin\frac{\eta}{2} \\ \cos\frac{\eta}{2} - \sin\frac{\eta}{2} & \cos\frac{\eta}{2} + \sin\frac{\eta}{2} \end{bmatrix}.$$

Thus, provided we calculate the density matrix in the stationary basis $\hat{\rho}$, we find it in the adiabatic basis $\hat{\rho}_{\text{adiab}}$,

$$\hat{\rho}_{\text{adiab}} = \hat{S}_2^{-1} \hat{\rho} \hat{S}_2. \qquad (18)$$

The initial condition for $\hat{\rho}$ can be obtained from the initial condition for $\hat{\rho}_{\text{adiab}}$ by inverting the relation (18).

Let us now consider as an illustrative example the one-sweep process,

$$t \in \left(-\frac{T}{4}, \frac{T}{4}\right), \quad T = \frac{2\pi}{\omega},$$

$$x(t) = x_0 \sin\omega t, \quad x(t) \in (-x_0, x_0), \quad x_0 \gg \Delta \gg \omega,$$

which corresponds to the LZ model [28]. We choose the initial condition to be

$$\hat{\rho}_{\text{adiab}}\left(-\frac{T}{4}\right) = \begin{bmatrix} 1 & 0 \\ 0 & 0 \end{bmatrix},$$

which means that the system at $t = -T/4$ is in the lower adiabatic state. We look for the occupation probability $P_\uparrow = \rho_{\text{adiab}}^{22}(t)$ of the upper adiabatic level $|\uparrow\rangle$, which equals to the LZ probability at the end of the sweep [28], $P_\uparrow(T/4) = P_{LZ}$. Thus, for the functions X, Y, Z, introduced in Sec. 2, we get the initial condition

$$X\left(-\frac{T}{4}\right) = \frac{x_0}{\sqrt{\Delta^2 + x_0^2}}, \qquad Y\left(-\frac{T}{4}\right) = 0,$$

$$Z\left(-\frac{T}{4}\right) = \frac{\Delta}{\sqrt{\Delta^2 + x_0^2}}$$

and find

$$P_\uparrow(t) = \frac{1}{2} - \frac{\Delta}{2\sqrt{\Delta^2 + x(t)^2}} Z(t) + \frac{x(t)}{2\sqrt{\Delta^2 + x(t)^2}} X(t).$$

This is illustrated in Fig. 1,b, which is equivalent to Fig. 3,d in Ref. 10.

In the general case, $x_{\text{off}} \neq 0$, we calculate $\hat{S}_2$ and then $\hat{\rho}_{\text{adiab}}$ according to Eq. (18). Then the probability $P_\uparrow$ is given by

$$P_\uparrow(t) = \frac{1}{2} - \frac{(\Delta^2 + x(t)x_{\text{off}})}{2\sqrt{\Delta^2 + x(t)^2}\sqrt{\Delta^2 + x_{\text{off}}^2}} Z(t) +$$

$$+ \frac{\Delta(x(t) - x_{\text{off}})}{2\sqrt{\Delta^2 + x(t)^2}\sqrt{\Delta^2 + x_{\text{off}}^2}} X(t).$$

This should be supplemented with the respective initial condition.

3.3. Crossover from multiphoton Rabi resonances to LZ-interferometry: numerical results

Now making use of the numerical solution of Eqs. (8)−(10) for the Hamiltonian (13), we study the dependence of the time-averaged probability $\overline{P}_+$ on frequency ω and amplitude x_0. For small amplitudes, $x_0 \ll \Delta E$, there are resonant peaks in the $\overline{P}_+ - \omega$ dependence at $\omega \simeq \Delta E/K$, as described in Sec. 3.1. and illustrated in Fig. 2. With increasing amplitude x_0, the resonances shift to higher frequencies. For $x_{\text{off}} = 0$, the resonances appear at «odd» frequencies ($K = 1, 3, 5, \ldots$) only, as was studied in Ref. 9. For $x_{\text{off}} \neq 0$ there are also resonances at «even» frequencies ($K = 2, 4, \ldots$), which is demonstrated in Fig. 2. We note that Fig. 2 is plotted for the ideal case of the absence of decoherence and relaxation, $\Gamma_\varphi = \Gamma_{\text{relax}} = 0$, when the resonant value is $\overline{P}_+ = 1/2$. The effect of finite dephasing, $\Gamma_\varphi \neq 0$, and relaxation, $\Gamma_{\text{relax}} \neq 0$, is to decrease the resonant values of $\overline{P}_+$ and to widen the peaks for $\Gamma_\varphi > \Gamma_{\text{relax}}$. Thus from the comparison of the theoretically calculated resonant peaks with the experi-
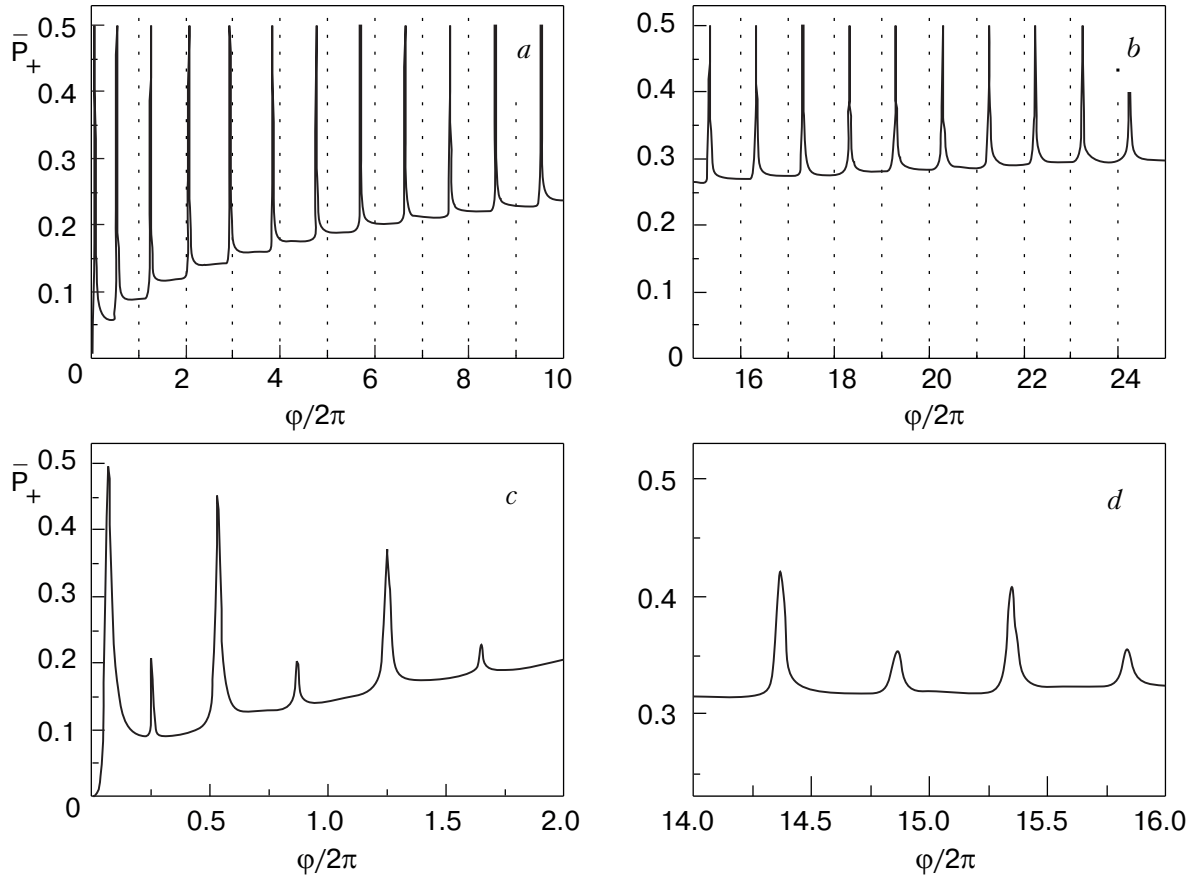
Fig. 3. Dependence of the probability $\overline{P}_+$ on $\varphi = 4x_0/\omega$ at $x_0\omega/\Delta^2 = 0.45$ (which corresponds to $P_{LZ} = 10^{-3}$); $\Gamma_\varphi = \Gamma_{\text{relax}} = 0$ and $x_{\text{off}} = 0$ for graphs (*a*) and (*b*); $\Gamma_\varphi/\Delta = \Gamma_{\text{relax}}/\Delta = 10^{-3}$ and $x_{\text{off}}/\Delta = 0.05$ for graphs (*c*) and (*d*).

mentally observed ones, the dephasing Γ_φ and the relaxation rates Γ_{relax} can be obtained [16].

When the system is driven slowly, $\omega \ll \Delta$, and with large amplitude, $x_0 \gg \Delta$, the LZ excitation mechanism is relevant for the description of the system dynamics. In the previous subsection we considered the LZ transition for a single-sweep event. Now we study the periodical driving of the system: interferences between multiple LZ transitions happen, which leads to resonant excitations [2,12,13]. We will compare these resonances with the multiphoton Rabi ones.

First, we note that the resonance positions depend on the amplitude; we demonstrate that for $\omega \ll \Delta < x_0$ in the inset of Fig. 2 . But it is more illustrative to study the resonance properties via the dependence of $\overline{P}_+$ on the ratio x_0/ω (or, more precisely, on the phase the state vector picks up per half-period [12] $\varphi = 4x_0/\omega$). It is reasonable to carry out the calculation for a fixed value of the product $x_0\omega$, which in its turn defines the LZ probability (see Eq. (17)). This allows us not only to compare our results with the results of Ref. 12, where the periodicity of the resonances in φ was predicted, but also to demonstrate the transition from the multiphoton Rabi resonances to the ones induced due

to the interference of LZ excitations by means of the $\overline{P}_+ - \varphi$ dependence.

In Fig. 3,*a*,*b* we plotted the dependence of $\overline{P}_+$ on φ for $x_{\text{off}} = 0$ and $\Gamma_\varphi = \Gamma_{\text{relax}} = 0$. The first few peaks, in the region $x_0 \lesssim \Delta$, corresponding to the multiphoton Rabi resonances are situated at $\varphi \sim K^2$ (that follows from the resonance relation $\omega = \Delta E/K$). With increasing φ (which is proportional to x_0) we observe the overall rising of the curve in accordance with the conclusions of Ref. 9. At $\varphi \gg 1$, i.e., at $\omega \ll \Delta \ll x_0$, the resonance position is 2π-periodic in agreement with Ref. 12. The nonzero offset $x_{\text{off}} \neq 0$ results in the appearance of additional resonances between the basic ones [12], which is demonstrated in Fig. 3,*c*,*d*. Such a feature is similar to the multiphoton Rabi resonances. Nonzero decoherence decreases and widens the peaks we have also demonstrated in Fig. 3,*c*,*d*.

In Fig. 4 we present the dependence of $\overline{P}_\uparrow$ on φ for the calculations carried out in the adiabatic basis (cf. Sec. 3.2.). In Fig. 4,*a*,*b* we plotted such a dependence for different values of φ at $x_{\text{off}} = 0$ and $\Gamma_\varphi = \Gamma_{\text{relax}} = 0$. For $\varphi \gg 1$ (see Fig. 4,*b*) the resonances are 2π-periodic, and the peaks are situated at the integer values of $\varphi/2\pi$, as predicted in Ref. 12. We also plotted the
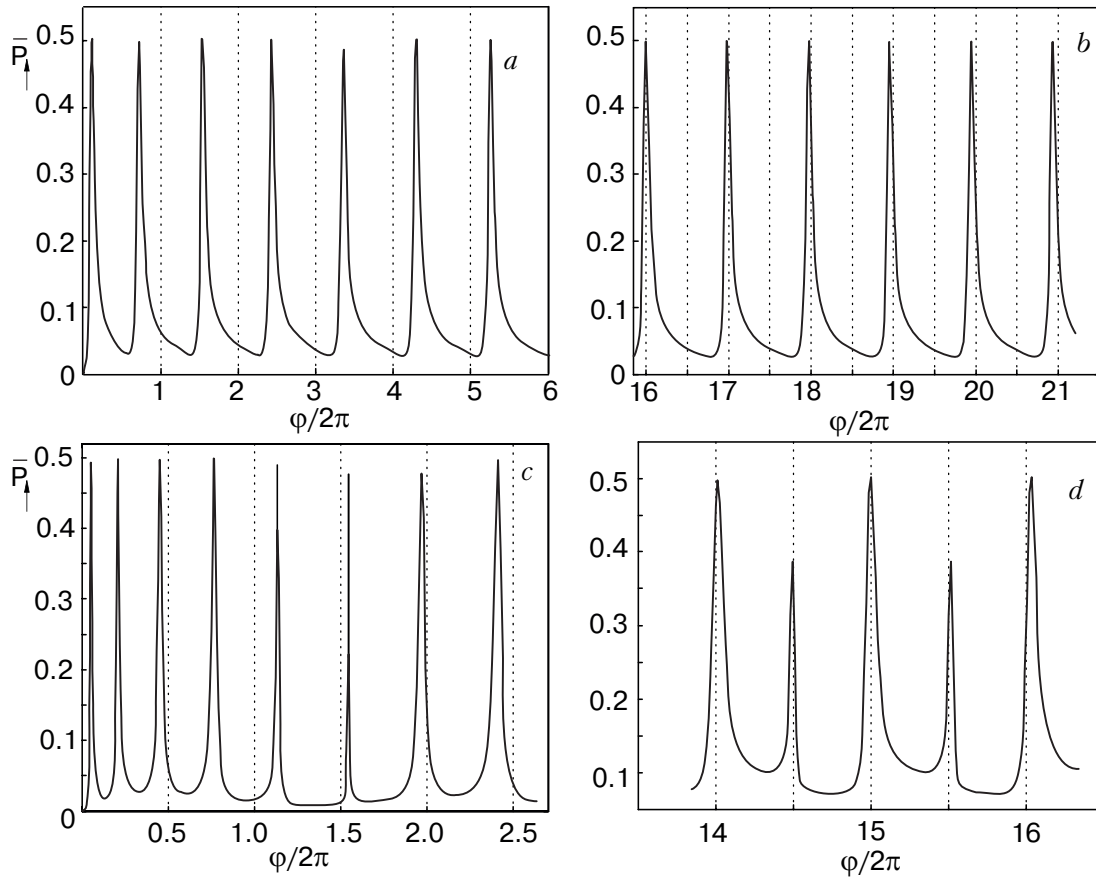
Fig. 4. The dependence of the probability $\overline{P}_\uparrow$ on the phase $\varphi = 4x_0/\omega$, $\Gamma_\varphi = \Gamma_{\text{relax}} = 0$ and $\varphi_{\text{off}} = 0$ for graphs (*a*) and (*b*), $\Gamma_\varphi = \Gamma_{\text{relax}} = 0$ and $\varphi_{\text{off}} = \pi/4$ for graph (*c*), $\Gamma_\varphi = 5\cdot10^{-4}$, $\Gamma_{\text{relax}} = 2.5\cdot10^{-4}$, $x_{\text{off}} = 0.35$ for graph (*d*).

dependence of $\overline{P}_\uparrow$ on φ for the nonzero offset $x_{\text{off}} \neq 0$ (see Fig. 4,*c*,*d*), namely for $\varphi_{\text{off}} = 4x_{\text{off}}/\omega = \pi/4$.

4. Multiphoton excitations in the interferometer-type charge qubit

4.1. Interferometer-type charge qubit

In this Section, we consider the quantum dynamics of the interferometer-type charge qubit with periodically varying control parameters [19–21]. This qubit consists of two Josephson junctions closed by a superconducting ring. The charge *en* of the island between the junctions is controlled by the gate voltage V_g via the capacitance C_g. The junctions are characterized by Josephson energies E_{J1}, E_{J2} and phase differences δ_1, δ_2. The relevant energy values are the island,s Coulomb energy, $E_C = e^2/2C_{\text{tot}}$, where C_{tot} is the total capacitance of the island, and the effective Josephson energy

$$\varepsilon_J = (E_{J1}^2 + E_{J2}^2 + 2E_{J1}E_{J2}\cos\delta)^{1/2}.$$

An important feature of the qubit is that its Josephson energy is controlled by the external magnetic flux Φ_e piercing the ring. In this paper, the ring

inductance L is assumed to be small. Then the total phase difference, $\delta = \delta_1 + \delta_2$, approximately equals to $\delta_e = 2\pi\Phi_e/\Phi_0$, and thus $\varepsilon_J = \varepsilon_J(\delta) \simeq \varepsilon_J(\delta_e)$.

Within the two-level model with the basis of «charge states» $|0\rangle$ and $|1\rangle$ corresponding to the excess number of Cooper pairs on the island, the Hamiltonian of the interferometer-type charge qubit can be written as [6]

$$\hat{H} = -\frac{1}{2}\varepsilon_J\hat{\sigma}_x - \frac{1}{2}E_{\text{ch}}\hat{\sigma}_z, \tag{19}$$

where $E_{\text{ch}} = 4E_C(1 - n_g)$ and $n_g = C_gV_g/e$. Here the domination of the Coulomb energy of a Cooper pair $4E_C$ over the coupling energy ε_J is assumed, $4E_C/\varepsilon_J > 1$. The eigenstates, $\{|-\rangle, |+\rangle\}$, of this Hamiltonian are discriminated by the direction of the supercurrent in the ring [21].

The qubit is considered to be coupled not only to the gate but also to the tank circuit that enables both phase control and readout. Thus there are two possibilities to make the Hamiltonian of the two-level system (19) time-dependent. First, the gate voltage V_g can be driven,

$$n_g = n_g^{(0)} + n_g^{(1)}\sin\omega t, \tag{20}$$

and, second, the dc and ac components of the current in the tank circuit can induce a periodically varying magnetic flux,

$$\delta = \delta_{dc} + \delta_{ac} \sin \omega t. \quad (21)$$

Here we restrict our consideration to the case of sinusoidal time dependence of the parameters.

Further we study the time-averaged occupation probability of the excited state $\overline{P}_+$. We note that because the two states $|-\rangle$ and $|+\rangle$ belong to oppositely circulating currents in the ring, they correspond to different signs of the qubit's Josephson inductance. The latter can be probed by the impedance measuring technique [25], which makes it possible to observe the resonant behaviour of $\overline{P}_+$ studied in the following subsection.

4.2. Resonant excitation of the interferometer-type charge qubit

The case of the excitation of the interferometer-type charge qubit via the gate (Eq. (20)) can easily be related to the one considered in Sec. 3; see the Hamiltonians (11) and (19) with the diagonal time-dependent parameters defined by Eq. (20). Then the ratio x_0/Δ is given by

$$\frac{x_0}{\Delta} = \frac{4E_C}{\varepsilon_J} n_g^{(1)}.$$

Thus, both mechanisms considered in Sec. 3 can be realized: multiphoton excitations ($x_0/\Delta \ll 1$) and LZ interferometry ($x_0/\Delta \gg 1$).

Let us now consider the second possibility of the excitation of the qubit by the time-dependent magnetic flux. The Hamiltonian of the interferometer-type charge qubit (19) with the periodically varying phase δ (Eq. (21)) is related to the Hamiltonian of a two-level system considered in Sec. 2 (Eq. (5)) by the following relations:

$$B_x(t) \equiv \varepsilon_J,$$

$$B_x^{(0)} = B_x(0) \equiv B_x|_{\delta_{ac}=0},$$

$$B_x^{(1)}(t) = B_x(t) - B_x(0),$$

$$B_z^{(0)} = E_{ch}.$$

In two limiting cases, the expressions can be simplified to result the time-dependent term in the form

$$B_x^{(1)}(t) \propto \sin \omega t. \quad (22)$$

Namely, for

$$\delta - \pi \gg \frac{|E_{J1} - E_{J2}|}{\sqrt{E_{J1}E_{J2}}}, \quad \delta_{ac} \lesssim \delta_{dc} - \pi \ll \pi \quad (23)$$

we have

$$B_x^{(0)} \simeq \sqrt{E_{J1}E_{J2}}(\delta_{dc} - \pi), \quad (24)$$

$$B_x^{(1)}(t) \simeq \sqrt{E_{J1}E_{J2}}\delta_{ac} \sin \omega t, \quad (25)$$

and for

$$\delta - \pi \ll \frac{|E_{J1} - E_{J2}|}{\sqrt{E_{J1}E_{J2}}}, \quad \delta_{ac} \ll \delta_{dc} - \pi \ll \pi, \quad (26)$$

it follows

$$B_x^{(1)}(t) \simeq |E_{J1} - E_{J2}|, \quad (27)$$

$$B_x^{(1)}(t) \simeq \frac{E_{J1}E_{J2}}{|E_{J1} - E_{J2}|}(\delta_{dc} - \pi)\delta_{ac} \sin \omega t. \quad (28)$$

When the relation (22) holds, the present problem (of the charge qubit with time-dependent magnetic control) can be related to the problem considered above in Sec. 3 by the expressions (6). Then we can estimate the ratio $x_0/\Delta E$, which characterizes the mechanism of the excitation of the qubit. For example, at $x_0/\Delta E \lesssim 1$ we expect multiphoton resonances in the qubit's response to the external alternating magnetic flux. We consider this case below in detail.

We note that the width of the resonant peaks is defined by the off-diagonal components of the Hamiltonian (13), i.e., by the product $x_0\Delta$. Then looking at Eqs. (25) and (28), we conclude that the width of the resonances is defined by the product $\delta_{ac}(1 - n_g)$.

Finally, we illustrate the multiphoton resonant excitations of the interferometer-type charge qubit.
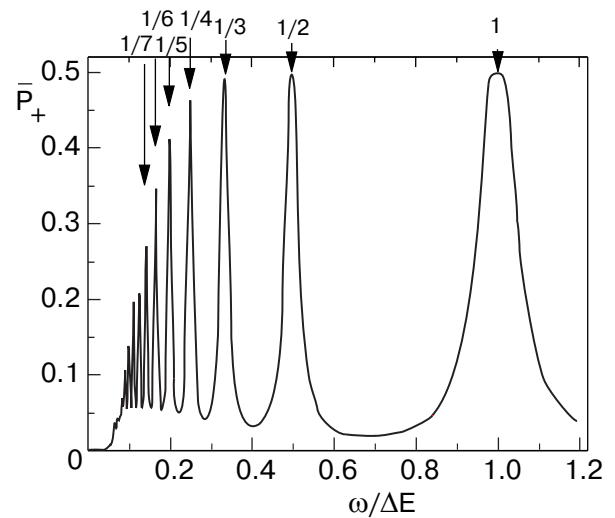

Fig. 5. Dependence of the probability $\overline{P}_+$ on the frequency ω for the phase-biased charge qubit at $n_g = 0.95$, $E_{J1}/E_C = 12.4$, $E_{J2}/E_C = 11$, $\Gamma_{relax}/E_C = 10^{-4}$, $\delta_{ac} = 0.2\pi$, $\delta_{dc} = \pi + 0.2\pi$.

Making use of the numerical solution of the master equation (Sec. 2), we find the time-averaged probability $\overline{P}_+$ plotted in Fig. 5. The position of the multiphoton resonant peaks is defined by the relation $\omega = \Delta E / K$, where $\Delta E = \Delta E(\delta_{dc})$ is supposed to be fixed. Alternatively, when the δ_{dc} component of the phase is changed and the frequency ω is fixed, a similar graph can be plotted with resonances at $\delta_{dc} = \delta_{dc}^{(K)}$ defined by the relation $\Delta E(\delta_{dc}^{(K)}) = K\omega$.

5. Conclusions

We have studied the dynamic behavior of a quantum two-level system subjected to periodic sweeping of its parameters. The energy levels population was calculated by solving the master equation for the density matrix with relaxation terms. Studying the population of the excited state in both stationary and adiabatic bases, we analyzed some features of the multiphoton Rabi and LZ effects. Particularly, we have shown certain similarities of the multiphoton resonances at $x_0 \ll \omega$ with the resonances at $x_0 \gg \Delta \gg \omega$ due to the interference between multiple LZ transitions. Based on the solution of the master equation for the density matrix, we described in detail the dynamic behaviour of the interferometer-type charge qubit subjected to periodically changing gate voltage or magnetic flux.

1. L.D. Landau, *Phys. Z. Sowjetunion* **2**, 46 (1932); C. Zener, *Proc. R. Soc. London, Ser. A* **137**, 696 (1932).
2. V.A. Benderskii, E.V. Vetoshkin, and E.I. Kats, *JETP* **97**, 232 (2003).
3. I.I. Rabi, *Phys. Rev.* **51**, 652 (1937).
4. N.B. Delone and V.P. Krainov, *Atoms in Strong Light Fields, Springer Ser. Chem. Phys.*, Vol. 28, Springer, Berlin-Heidelberg (1985) (also in Russian: *Atom v sil'nom svetovom pole*, Atomizdat, Moscow (1978)).
5. M. Grifoni and P. Hänggi, *Phys. Rep.* **304**, 229 (1998).
6. Yu. Makhlin, G. Schön and A. Shnirman, *Rev. Mod. Phys.* **73**, 357 (2001).
7. Y. Nakamura, Yu.A. Pashkin, and J.S. Tsai, *Nature* **398**, 786 (1999).
8. J.E. Mooij, T.P. Orlando, L. Levitov, Lin Tian, Caspar H. van der Wal, and Seth Lloyd, *Science* **285**, 1036 (1999).
9. V.P. Krainov and V.P. Yakovlev, *Sov. Zh. Exp. Theor. Fiz.* **78**, 2204 (1980).
10. N.V. Vitanov, *Phys. Rev.* **A59**, 988 (1999).
11. D.A. Garanin and R. Schilling, *Phys. Rev.* **B66**, 174438 (2002).
12. A.V. Shytov, D.A. Ivanov, and M.V. Feigel'man, *Europhys.* **B36**, 263 (2004).
13. Y. Teranishi and H. Nakamura, *Phys. Rev. Lett.* **81**, 2032 (1998).
14. Y. Nakamura, Yu.A. Pashkin, and J.S. Tsai, *Phys. Rev. Lett.* **87**, 246601 (2001).
15. J.Q. You and F. Nori, *Phys. Rev.* **B68**, 064509 (2003).
16. S. Saito, M. Thorwart, H. Tanaka, M. Ueda, N. Nakano, K. Semba, and H. Takayanagi, *Phys. Rev. Lett.* **93**, 037001 (2004).
17. D. Born , V.I. Shnyrkov, W. Krech, Th. Wagner, E. Il'ichev, M. Grajcar, U. Hübner, and H.-G. Meyer, *Phys. Rev.* **B70**, 180501(R) (2004).
18. G. Falci, R. Fazio, G.M. Palma, J. Siewert, and V. Vedral, *Nature* **407**, 355 (2000).
19. A.B. Zorin, *Physica* **C368**, 284 (2002).
20. J.R. Friedman and D.V. Averin, *Phys. Rev. Lett.* **88**, 050403 (2002).
21. W. Krech, M. Grajcar, D. Born, I. Zhilyaev, Th. Wagner, E. Il'chev, and Ya. Greenberg, *Phys. Lett.* **A303**, 352 (2002).
22. K. Blum, *Density Matrix Theory and Applications*, Plenum Press, New York−London (1981).
23. The phenomenological description of the relaxation processes in terms of the rates was shown [12] to be equivalent to the microscopic description which intrinsically includes the reservoir. Such a phenomenological approach was successfully applied to the description of the quantum dynamics of phase qubits [16].
24. A. Aassime, G. Johansson, G. Wendin, R.J. Schoelkopf, and D. Delsing, *Phys. Rev. Lett.* **86**, 3376 (2001).
25. E. Il'ichev, N. Oukhanski, Th. Wagner, H.-G. Meyer, A.Yu. Smirnov, M. Grajcar, A. Izmalkov, D. Born , W. Krech, and A. Zagoskin, *Fiz. Nizk. Temp.* **30**, 823 (2004) [*Low Temp. Phys.* **30**, 620 (2004)].
26. S. Flügge, *Practical Quantum Mechanics* II, Springer, Berlin−Heidelberg−New York (1971), task 180.
27. C. Cohen-Tannoudji, J. Dupont-Roc, and G. Grynberg, *Atom-Photon Interactions*, Wiley, New York (1992).
28. In the vicinity of the transition point $x = 0$ (where the excitation happens), $x(t)$ is a linear function of t, $x(t) \simeq x_0 \omega t$, which is exactly the LZ model. Deviations of the function $x(t)$ from the linear dependence far from the transition point do not matter [11]. This explains the quantitative coincidence of the results presented in this section with the results obtained with $x(t)$ being a linear function.